Porous Fluorinated Aluminum and Mixed Gallium/Aluminum Oxide Pillared Tin Phosphate Materials with Acid Properties

Pilar Braos-García, Enrique Rodríguez-Castellón, Pedro Maireles-Torres, Pascual Olivera-Pastor, and Antonio Jiménez-López*

Departamento de Química Inorgánica, Cristalografía y Mineralogía, Facultad de Ciencias, Universidad de Málaga, Campus de Teatinos, 29071-Málaga, Spain

Received: September 29, 1997; In Final Form: December 18, 1997

Fluorinated aluminum and mixed gallium/aluminum oligomers of high nuclearity have been intercalated into α-tin phosphate by refluxing fluorinated Al and mixed Ga/Al oligomeric solutions in the presence of colloidal tin phosphate. ^{31}P and ^{27}Al MAS NMR spectroscopy has revealed the existence of strong interactions between the phosphate layers and the oligomeric guest species, conferring to these expanded materials a high thermal stability, as confirmed by XRD studies. Formation of Al and mixed Ga/Al oxide nanoparticle pillars in the interlayer region of tin phosphate, upon calcination at 400 °C, gave rise to porous materials with specific surface areas between 160 and 304 $m^2\ g^{-1}$ and micropore volumes close to 0.1 $cm^3\ g^{-1}$. The pillared materials are highly acidic solids and behave as dehydrating catalysts for the decomposition reaction of isopropyl alcohol. The Lewis acid sites, believed to be mainly responsible for the catalytic activity, are associated with low coordination sites of Al ions present in the interlayer oxide pillars.

Introduction

A vast majority of works on pillared structured solids are devoted to the synthesis and characterization of clays,[1] phosphates[2] and other hosts[3] pillared with the well-known aluminum polyoxocation, $[AlO_4Al_{12}(OH)_{12}(H_2O)_{24}]^{7+}$, ($Al_{13}^{7+}$), which consists of a central tetrahedral aluminum surrounded by 12 edge-sharing octahedral aluminums.[4] The products obtained exhibit properties, such as surface area, pore size, and acidity, which can be tuned by adequate choice of reactants and experimental conditions. The similarity between the hydrolysis behavior of Al^{3+} and Ga^{3+} ions has also led to the study of mixed Ga/Al oligomeric species.[5] The most relevant finding was that $GaAl_{12}$ possessed a much higher thermal stability than Al_{13} and Ga_{13} homologues and presented a similar Keggin-type structure with Ga ions in the tetrahedral sites, as demonstrated by X-ray diffraction and NMR spectroscopy. Indeed, the intercalation of $GaAl_{12}$ species in clays has provided pillared solids with basal spacings close to that obtained with Al_{13} oligomers and specific surface areas which were preserved at temperatures where alumina pillared clays collapsed. These studies have demonstrated, therefore, the high thermal and hydrothermal stability of $GaAl_{12}$-pillared clays and, moreover, the presence of strong acid sites in these materials which results, for instance, in better selectivity for the isomerization of *n*-heptane.[6]

Likewise, layered metal(IV) phosphates are, by their properties as ion exchangers and catalysts, adequate candidates for intercalating many different oligomeric species.[7] The synthesis, characterization, and applications of nanostructured inorganically pillared layered metal(IV) phosphates have been very recently reviewed.[8] Precedent studies have demonstrated that species larger than the Al_{13}^{7+} ion are needed for generating interlayer porosity in α-zirconium phosphate, in order to balance the strong interaction established between the phosphate layer and the oxide nanoparticles acting as pillars, which favors the formation of stuffed structures.[9] These studies also revealed that the incorporation of F^- ions into intercalated clusters was beneficial in order to improve porosity and thermal stability of the pillared materials. The question arises whether M(IV) phosphates can develop interlayer porosity by intercalation of large fluorinated species, formed by not only aluminum but also mixed species, such as Ga/Al. This method of intercalation may thereby open new possibilities for preparation of a great number of aluminum-based oxide pillared materials with tunable surface properties by appropriate choice of the composition of mixed species and experimental conditions.

The purpose of the work reported in this paper was to synthesize porous materials based on aluminum and mixed gallium/aluminum pillared α-tin phosphate intercalation compounds, by using solutions containing fluorinated Al or mixed Ga/Al clusters of high nuclearity. Characterization of the intercalates and calcined materials was carried out by chemical analyses, X-ray diffraction, TGA-DTA, XPS, ^{31}P and ^{27}Al solid-state MAS NMR, N_2 adsorption−desorption (at 77 K), temperature-programmed desorption of NH_3, and the catalytic decomposition of isopropyl alcohol.

Experimental Section

Materials. Colloidal suspensions of tetramethylammonium−tin phosphate (TMA−SnP) were synthesized as follows: 5 g of α-SnP, prepared according to the Costantino and Gasperoni method,[10] was dispersed in 355 mL of a 0.06 M solution of *n*-propylamine (NPA) in *n*-hexane (corresponding to the 70% of the cation exchange capacity of α-tin phosphate), and the solution was stirred for 2 h at room temperature. The solid, recovered by centrifugation and air-dried, was then added to 122 mL of a 2.5 M aqueous solution of tetramethylammonium chloride (TMA−Cl), maintained for 1 day under stirring at room temperature, and finally the suspension was centrifuged and the solid washed with water and air-dried at 60 °C.

S1089-5647(97)03168-4 CCC: $15.00
Published on Web 02/14/1998

TABLE 1: Surface (XPS) Atomic Ratios, d_{00l} Spacings, and Chemical Formulas for the Studied Precursor Samples

sample	surface[a] F/M	surface[a] Ga/Al	d_{00l}/Å rt	d_{00l}/Å 400 °C	chemical formulas[b]
Al−SnP	0.45		23.4	17.5	$Sn[Al_{24}O_8(OH)_{46}(H_2O)_{18}]_{0.14}H_{0.6}(PO_4)_2 \cdot 7.3H_2O$
$GaAl_{13}$−SnP	0.50	1/9	23.0	16.7	$Sn[Ga_{1.75}Al_{22.25}O_8(OH)_{46}(H_2O)_{18}]_{0.13}H_{0.7}(PO_4)_2 \cdot 4.6H_2O$
Ga_3Al_{11}−SnP	0.36	3/8	29.3	21.6	$Sn[Ga_{6.02}Al_{17.98}O_8(OH)_{46}(H_2O)_{18}]_{0.16}H_{0.4}(PO_4)_2 \cdot 7.9H_2O$
Ga_6Al_7−SnP	0.13	6/1	23.4	16.3	$Sn[Ga_{17.66}Al_{6.34}O_8(OH)_{46}(H_2O)_{18}]_{0.12}H_{0.8}(PO_4)_2 \cdot 7.3H_2O$

[a] From XPS analysis (M = Al + Ga). [b] Al and Ga/Al expressed as the $[Al_{24-x}Ga_xO_8(OH)_{46}(H_2O)_{18}]^{10+}$.

The oligomeric aluminum solution was prepared according to the procedure described by Fu et al.[11] Al foil was dissolved in an $AlCl_3$ aqueous solution under reflux for 2 days (final concentration of Al was equal to 1 M). In the case of mixed oligomeric aluminum−gallium solutions, Al foil was treated with a mixture of $AlCl_3$ and $GaCl_3$, to achieve final Ga/Al molar ratios of 1/12, 3/10, and 6/7, under reflux for 1 day (final concentration of (Al + Ga) = 0.4 M). In all cases, the $GaCl_3$ solutions were prepared by treating metallic gallium in a concentrated 3:1 HCl/HNO_3 mixture (HCl/Ga molar ratio being 3:1). A tetramethylammonium fluoride solution was finally added to each solution to attain $F^-/(Al^{3+} + Ga^{3+})$ molar ratios lower than 0.5. Aliquots of these oligomeric solutions, corresponding to 6.90 mmol of M_2O_3/g of SnP_2O_7 (M = Al, Ga), were added to a colloidal aqueous suspension of TMA−SnP (2 wt %). The resulting suspensions were refluxed for 1 day, centrifuged, water-washed, and air-dried. Intercalation compounds (precursors), hereafter designated as Al−SnP, $GaAl_{13}$−SnP, Ga_3Al_{11}−SnP, and Ga_6Al_7−SnP, were finally calcined in air at 400 °C during 6 h.

Chemical Analyses and Characterization. Chemical analyses of the synthesized materials were carried out after digestion in 60% HNO_3 for 1 day and hot 1 M NaOH for 4 days. The concentrations of Al and Ga were determined by atomic absorption with a Perkin-Elmer 400 A.A. spectrometer.

XRD of samples as cast films was recorded on a Siemens D501 diffractometer using Cu Kα radiation and a graphite monochromator. Thermogravimetric (TG) and differential thermal analyses (DTA) were carried out with a Rigaku Thermoflex TG 3110 instrument (calcined Al_2O_3 as a reference and 10 °C min^{-1} heating rate).

X-ray photoelectron spectra (XPS) were recorded with a Physical Electronics 5700 spectrometer equipped with a dual X-ray excitation source (Mg Kα, $h\nu$ = 1253.6 eV, and Al Kα, $h\nu$ = 1486.6 eV) and multichannel hemispherical electron analyzer. The samples were turbopumped to ca. 10^{-9} Torr before they were moved into the analysis chamber. The residual pressure in this ion-pumped chamber was maintained below 10^{-9} Torr during data acquisition. The binding energies were obtained with an accuracy of ±0.1 eV and by charge referencing to the adventitious C 1s peak at 284.8 eV.

The MAS NMR spectra were recorded on a Bruker AMX 300 spectrometer equipped with a multinuclear probe. Powder samples were packed in zirconia rotors. For ^{27}Al, samples were spun at 3.0 kHz, and spectra recorded at 78.23 MHz, using a pulse width of 3 μs, a spectral width of 50 kHz, a recycle delay of 0.3 s, 10 000 scans, and 10 Hz exponential line broadening. Chemical shifts are reported in ppm from H_3PO_4 and $[Al(H_2O)_6]^{3+}$ solutions.

Adsorption−desorption isotherms of N_2 at 77 K of calcined samples were obtained in a conventional volumetric apparatus, after outgassing of samples at 200 °C (10^{-4} Torr overnight). BET specific surface areas were evaluated using 0.162 nm^2 as the cross-sectional area of the adsorbed N_2 molecule. Pore size distributions were calculated by the use of the Cranston and Inkley method for cylindrical pores.[12]

The total acidity of the calcined samples was determined by temperature-programmed desorption of ammonia (NH_3 TPD). Before the adsorption of ammonia at 100 °C, samples were treated under helium at 400 °C for 1 h. The desorption of ammonia was run between 100 and 400 °C, at 10 °C min^{-1}, and analyzed in an on-line gas chromatograph (Shimadzu 6C-14A) provided with a thermal conductivity detector.

Catalytic Activity Measurements. The catalytic activity of the pillared solids in the decomposition of isopropyl alcohol was tested in a fixed-bed tubular glass reactor at atmospheric pressure and 220 °C, with a catalyst charge of 20 mg without dilution. The feed was a mixture of isopropyl alcohol in He obtained by passing a flow of He through isopropyl alcohol (chromatographic purity grade) held in a saturator−condenser kept at 30 °C. A constant total flow of 4.17×10^{-7} m^3 s^{-1} with an alcohol concentration of 11.3 vol % was used, with a spatial velocity of 83.5 μmol s^{-1} g^{-1}. Catalysts did not show diffusional restrictions. Prior to catalytic tests, carrier gas was passed through a molecular sieve, and the samples were pretreated under a He flow at 220 °C for 2 h. The reaction products were analyzed in an on-line gas chromatograph with a flame ionization detector and fused silica column SPB1.

Results and Discussion

Intercalation of Al and Mixed Ga/Al Oligomers. Previous studies have demonstrated that the colloidal intermediate phase of tetramethylammonium−tin phosphate (TMA−SnP) is appropiate for the intercalation of metal oligomeric species.[13] The preparation of this colloidal phase requires a previous intercalation of *n*-propylamine and then to exchange the interlayer *n*-propylammonium ions formed by tetramethylammonium. In the present work, *n*-hexane was used as solvent for intercalating *n*-propylamine in order to minimize the hydrolysis of tin phosphate, which is a major drawback in neutral and basic aqueous media.[14]

Prior to the intercalation reaction, the oligomeric solutions were aged at reflux conditions, and subsequently a tetramethylammonium fluoride aqueous solution was added at room temperature in order to form large oligomeric species. This addition of fluoride was necessary to improve the thermal stability of intercalated oligomers and avoid competition of aluminum monomers, by removing them as AlF_6^{3-}.[9] The fluorinated Al− and Ga/Al−tin phosphate precursor solids are obtained by slow addition of aliquots of fluorinated oligomeric solutions to colloidal TMA−SnP and refluxing the mixture for 1 day. Chemical compositions of the precursor Al− and Ga/Al−SnP materials are shown in Table 1. Bulk Ga/Al analyses are close to nominal values, except for Ga_6Al_7−SnP solid in which a very low uptake of Al is detected. In this sample, the total uptake is the lowest (4.84 mmol of M_2O_3 g^{-1} of SnP_2O_7), whereas the other samples exhibit values similar to that of fluorinated Al−SnP material. A comparison of the bulk and

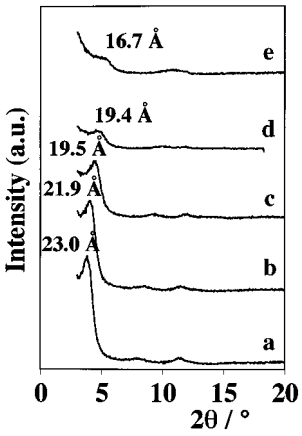

Figure 1. XRD patterns of $GaAl_{13}$−SnP at different temperatures: (a) room temperature, (b) 100 °C, (c) 200 °C, (d) 300 °C, and (e) 400 °C.

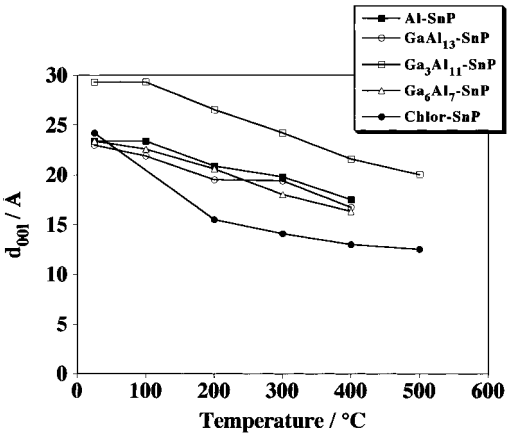

Figure 2. Evolution of the basal spacing, d_{00l}, with temperature for fluorinated Al− and Ga/Al−SnP intercalates: (a) Al−SnP, (b) $GaAl_{13}$−SnP, (c) Ga_3Al_{11}−SnP, (d) Ga_6Al_7−SnP, and (e) Chlorhydrol−SnP.

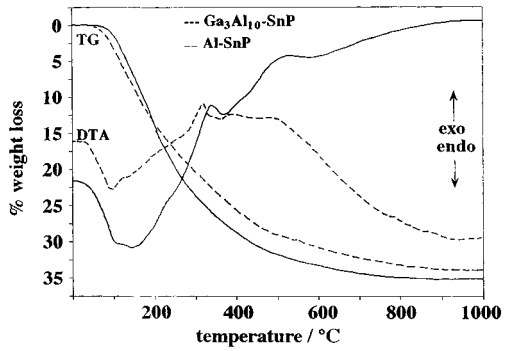

Figure 3. TG and DTA curves of fluorinated Al−SnP and Ga_3Al_{11}−SnP materials.

surface (XPS) Ga/Al ratios with the added Ga/Al ratios reveals that, at least, for Ga/Al ratios ≤3/10 the composition of the intercalated oligomeric species does not deviate appreciably from the initial composition of the oligomeric solution, and moreover, mixed oligomers are inserted into the phosphate interlayer region, as no significant variations between the bulk and surface ratios are found. However, upon increasing the relative concentration of Ga in solution, the composition of the intercalated oligomers is strongly enriched in Ga. This may be due to mixed oligomers with intermediate compositions having a very low stability, as a consequence of the difference of size between Ga^{3+} and Al^{3+} ions, which must cause strong distortions in the mixed oligomeric structure. In any case, the affinity of the phosphate layers seems to be higher for mixed species with high Ga content, which may be related to the trend of aluminum to bond preferentially to fluoride ions. This is confirmed by the fact that the highest fluoride content corresponds to the intercalated mixed oligomers with the highest Al content (Table 1).

The XRD data for the intercalated compounds at room temperature reveal that oligomers with similar size were intercalated in samples Al−, $GaAl_{13}$−, and Ga_6Al_7−SnP. The d_{00l} basal spacings of these samples, 23−23.4 Å, are slightly higher than that of the analogous fluorinated Al−ZrP material,[9] which means that species with similar nuclearity are intercalated in both phosphates using the same intercalation method. This difference could be a consequence of the hydrothermal treatment (200 °C) of the latter. The corresponding gallery height values, obtained by subtracting the layer thickness (∼6.5 Å) to the d_{00l} spacing, are in the range 16.5−16.9 Å, much higher than that expected for the intercalation of a monolayer of the Al_{13}^{7+} ions, which have a prolate form with a major axis of ∼9.5 Å.[4] The sample Ga_3Al_{11}−SnP exhibits the highest basal expansion yet observed for intercalation compounds of metal(IV) phosphates containing aluminum species. Upon heating, the intercalated materials undergo a gradual decrease of the d_{00l} spacing and a progressive amorphization (Figures 1 and 2), but high basal expansions are still maintained at 400 °C (Table 1) and the crystallinity is completely lost beyond 500 °C. In any case, XRD data suggest that both Al and mixed Ga/Al species intercalated into the layered tin phosphate show higher nuclearity than the tridecameric species, usually found in the interlayer region of pillared smectites. This is mainly attributed to the fact that the reflux method used favors coalescence of the Keggin ion.[1h] In addition, the presence of F^- prevents any competition of low nuclearity species.

The thermal behavior of these intercalation compounds is significantly different from that of the Chlorhydrol−SnP material, prepared by adding a Chlorhydrol solution to colloidal tin phosphate at room temperature.[13a] The former display much higher thermal stability than the latter, despite the basal spacing at room temperature of this solid being compatible with the presence of a bilayer of Al_{13}^{7+} ions. In particular, the free height of sample Ga_3Al_{11}−SnP is about 10 Å higher than that of Chlorhydrol−SnP at 500 °C. The high thermal stability showed by fluorinated Al- and mixed Ga/Al oligomer intercalated materials as compared with Chlorhydrol−SnP may be attributed to (i) the presence of species larger than Al_{13}, which might be formed by condensation of incomplete units derived from the Keggin ion framework,[11] and (ii) the partial replacement of OH^- groups by F^- ions in the oligomeric framework, which diminishes the possibility of condensation of M−OH groups from the oligomers with P−OH groups from the phosphate layer and, thus, retards spreading of the intercalated species throughout the phosphate interlayer region.

Thermogravimetric and differential thermal analyses (TG-DTA) of fluorinated Al− and Ga/Al−SnP materials show transitions at similar temperatures (Figure 3). The first endothermic effect in the DTA curve centered at 69−76 °C is assigned to the loss of waters of hydration, and the second one at 108−125 °C could correspond to the removal of coordinated water molecules. However, these two phenomena are not well differentiated in the TG curves, where a continuous weight loss is observed, extending from room temperature to ca. 700 °C which may also include the dehydroxylation of the oligomers and condensation with the phosphate layers. A characteristic exothermic effect, at temperatures higher than 800 °C, corresponding to the phase transition from layered to cubic tin

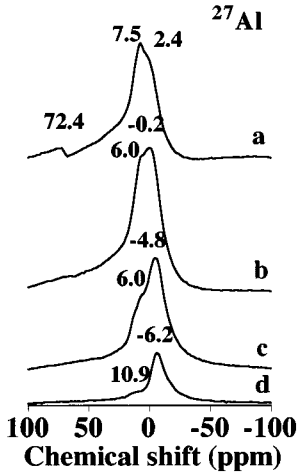

Figure 4. ^{27}Al MAS NMR spectra of fluorinated precursor materials: (a) Al−SnP, (b) $GaAl_{13}$−SnP, (c) Ga_3Al_{11}−SnP, and (d) Ga_6Al_7−SnP.

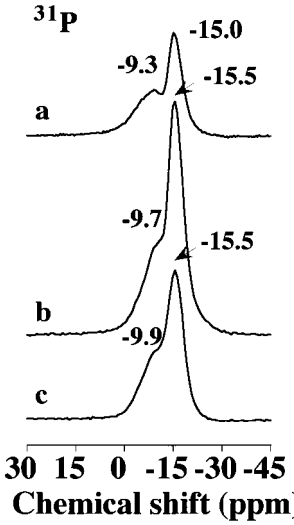

Figure 5. ^{31}P MAS NMR spectra of fluorinated precursor materials: (a) Al−SnP, (b) $GaAl_{13}$−SnP, and (c) Ga_3Al_{11}−SnP.

pyrophosphate is not observed in any case. This is attributed to the existence of strong interactions between metal oxide pillars and phosphate groups in the interlayer region, thus avoiding collapse of the layers. Hydration and coordination water range between 27 and 31 wt %, and in all cases, a small proportion of organic matter is still present.

MAS NMR spectroscopy has been utilized in order to elucidate the chemical nature of the intercalated Al− and Ga/Al oligomers and the types of interactions between the phosphate groups and the guest species. A study by ^{27}Al NMR and powder X-ray diffraction on kinetics of formation in solution of Al_{13}, hybrid MAl_{12} species, and larger oligomers has been very recently reported.[15] At high temperature, the polynuclear species, so-called AlP_2, which is thought to be formed by condensation of two Al_{12} units, resulting from the loss of an $Al(H_2O)_6^{3+}$ monomer in the tridecameric structure, was found in solution, confirming previous work reported by others.[11] However, it seems that the presence of Ga^{3+} in Al^{3+} solution favors the formation of $GaAl_{12}$ species against polymerization.

Figure 4 shows the ^{27}Al MAS NMR spectra of fluorinated Al− and Ga/Al−SnP intercalates. In the spectrum of the fluorinated Al−SnP solid, a resonance band appears at 72.4 ppm, practically in the same position as that of tetrahedral aluminum (Al_{IV}) in AlP_2 clusters.[11] As gallium is added, this signal disappears probably due to the tendency of Ga to occupy first the tetrahedral positions in the Keggin ion framework, forming the most thermodynamically favored $GaAl_{12}$ species. In the region corresponding to octahedral aluminum (Al_{VI}), two maxima at −6.2 to 2.4 and 6.0 to 10.9 ppm can be distinguished. This splitting of the Al_{VI} signal is probably a consequence of the interaction of the intercalated oligomers with the phosphate layer.

^{31}P MAS NMR spectra of Al− and Ga/Al−SnP intercalates are displayed in Figure 5. The ^{31}P chemical shift (δ), which appears at −12.5 ppm in α-SnP,[16] is split into two peaks upon intercalation of the oligomeric species of aluminum, the most intense centered at −15.0 ppm and the second at −9.3 ppm. The first resonance, according to previous work,[17] is assigned to phosphate groups interacting with aluminum oligomers. The shift toward higher field positions may be attributed to the increase of cation charge around the phosphorus tetrahedra upon interaction with Al oligomers. On the other hand, the peak at lower field, between −9.3 and −9.9 ppm, may correspond to deprotonated phosphate groups which are more distant from the interlayer oligomeric species. This signal has been also observed in the spectra of *n*-propylamine metal(IV) phosphate intercalates, where the interaction between $P-O^-$ and $^+NH_3-R$ groups was postulated.[18] The presence of Ga atoms in the mixed oligomeric species only leads to slight changes in the ^{31}P MAS NMR spectra which suggest that the intercalated mixed Ga/Al oligomers are structurally analogous to the Al species, with the gallium ions first occupying the central tetrahedral position and then the octahedral sites. It seems, therefore, that the presence of the phosphate induces the condensation of $GaAl_{12}$ units, present initially in solution, to form more bulky species which are intercalated in the interlayer region.

Pillared Materials. The Al− and Ga/Al oxide pillared materials were obtained by calcining the precursor solids at 400 °C in air. Transformation of intercalated oligomers into oxide nanoparticles causes, as mentioned above, a partial shrinkage of the interlayer region, but these materials still maintain large spacings between 10.2 and 15.1 Å (Table 1). The absence of reflection lines corresponding to Al or mixed Ga/Al oxides in the X-ray diffraction patterns of fluorinated Al− and Ga/Al−SnP materials indicates that no precipitation of the metal hydroxides took place during the intercalation process of the metallic oligomers.

The binding energy (BE) values of P(2p) and Sn($3d_{5/2}$) for these materials range between 133.6−134.5 and 486.5−487.1 eV, respectively. They are similar to those found in chromia-pillared SnP materials.[19] The O(1s) BE values occur between 530.9 and 531.8 eV and are comparable to those of α-SnP (531.8 eV) and Al_2O_3 (531.8 eV) but significantly lower than those reported for aluminum phosphates (532.8 eV); thus, the formation of a segregated $AlPO_4$ phase during the pillaring process may be ruled out.[20] On the other hand, F^- is an anion of very strong affinity for Al^{3+} and thus may cause a break of the Al−OH bond and act as a ligand in the oligomeric framework by partially substituting OH^- groups. The F(1s) BE (684.4−684.8 eV) of pillared materials is consistent with this partial substitution of OH^- for F^-, as the values found were intermediate between those corresponding to ionic (e.g., 684.5 eV for NaF) and covalent (e.g., 685.5 eV for AlF_6^{3-}) fluorides. Although Al^{3+} displays a higher affinity for F^- than Ga^{3+}, the existence of Ga−F bonds in the mixed Ga/Al oligomers cannot be ruled out since the BE of gallium fluoride compounds is also close to 685 eV.[20]

Concerning the ^{27}Al MAS NMR spectra of pillared materials (Figure 6), the most relevant feature is the presence of a new

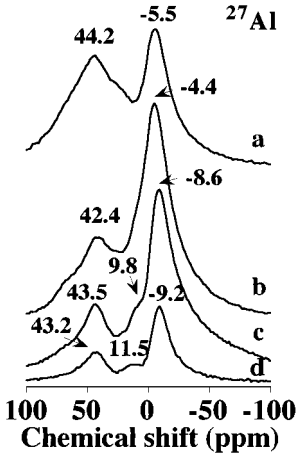

Figure 6. ^{27}Al MAS NMR spectra of fluorinated calcined materials: (a)−(d) as in Figure 4.

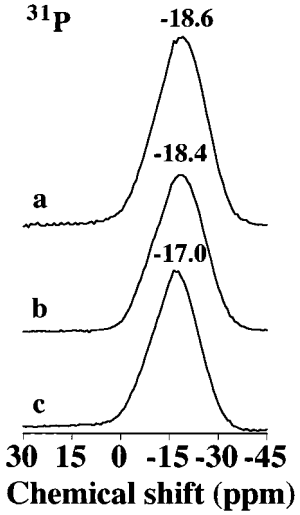

Figure 7. ^{31}P MAS NMR spectra of fluorinated calcined materials: (a)−(c) as in Figure 5.

broad band, especially intense in the fluorinated Al−SnP sample, at 44.2 ppm which cannot be unambiguously assigned to distorted tetrahedral or pentacoordinated aluminum, but in any case, it would mean that cross-linking between oxide pillars and the phosphate layers causes a decrease in the coordination number of the aluminum ions directly bonded to the layer.[9,17] This evolution of the ^{27}Al MAS NMR spectra with temperature is similar to that reported for the AlP_2 species, where the signals of Al_{IV} and Al_{VI} vanish at the same time as a new resonance, attributed to pentacoordinated aluminum, appears at 35 ppm, becoming dominant at higher temperature.[21,22] On the other hand, Mortlock et al. have observed that the signal of pentacoordinated aluminum shifts downfield, near 45 ppm, upon linking to phosphate ions.[23] Calcination of hydroxy−Al pillared montmorillonite and beidellite also gives rise to the appearance of a signal near 35 ppm.[6c] The existence of Al ions in low coordination environments is important from a catalytic viewpoint, because they act as Lewis acid sites.

The ^{31}P MAS NMR spectra of calcined materials are shown in Figure 7. After calcination at 400 °C, the resonance at −9.6 ppm disappears, whereas the signal at higher field is broadened and simultaneously moves to upfield and is now centered between −17.0 and −18.6 ppm. These changes are in line with a strong interaction between the intercalated species and the phosphate layers, possibly established through P−O−Al bonds.

Unlike what happens upon calcining Cr(III) polyhydroxocation intercalates, where segregated phases of Cr_2O_3 and cubic SnP_2O_7 were detected,[13b] the strong interaction between the aluminum-containing species and the phosphate groups leads finally to the breakup of the layered tin phosphate structure and subsequent formation of aluminum and/or gallium phosphate upon calcination at 1000 °C. The corresponding XRD patterns show peaks characteristic of SnO_2 (3.35, 2.64, and 2.37 Å) and gallium/aluminum phosphates (4.13, 3.57, 2.53, and 2.16 Å).

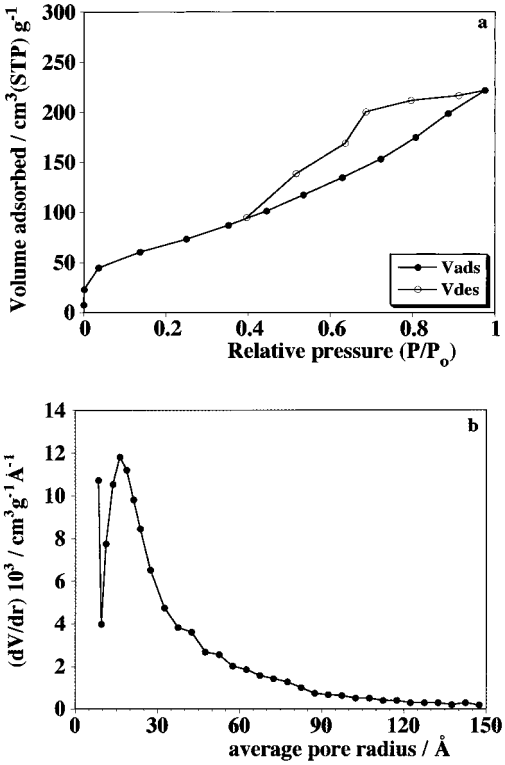

Figure 8. (a) N_2 adsorption−desorption isotherm and (b) pore size distribution for sample Ga_3Al_{11}−SnP.

TABLE 2: Textural Parameters of Fluorinated Al− and Ga/Al Pillared Tin Phosphate Materials

sample	S_{BET}[a] ($m^2\,g^{-1}$)	$\sum S_{ac}$[b] ($m^2\,g^{-1}$)	$\sum V_p$[b] ($cm^3\,g^{-1}$)	d_p(av)[b] (Å)	V_μ[c] ($cm^3\,g^{-1}$)
Al−SnP	304	400	0.478	48	0.104
$GaAl_{13}$−SnP	187	264	0.332	50	0.075
Ga_3Al_{11}−SnP	243	300	0.357	48	0.093
Ga_6Al_7−SnP	160	198	0.241	49	0.064
Chlor−SnP[d]	190	141	0.295	84	0.019

[a] BET specific surface area. [b] Accumulated surface area ($\sum S_{ac}$), pore volume ($\sum V_p$), and average pore diameter (d_p(av)) calculated by Cranston and Inkley's method. [c] Micropore volume, calculated by Dubinin−Radushkevich's equation. [d] From ref 13a.

Textural properties of fluorinated aluminum− and gallium/aluminum oxide pillared tin phosphate materials have been evaluated by N_2 adsorption−desorption at 77 K. The corresponding isotherms (Figure 8) are typical of mesoporous solids with a certain contribution of micropores. The textural parameters are summarized in Table 2, as well as those of Chlorhydrol−SnP calcined at 400 °C, for comparison. Although α-SnP itself is a nonporous solid, with a BET specific surface area close to 10 $m^2\,g^{-1}$, the pillared materials are porous materials having S_{BET} values between 160 and 304 $m^2\,g^{-1}$. The most porous material is Al−SnP with a S_{BET} of 304 $m^2\,g^{-1}$ and a pore volume of 0.478 $cm^3\,g^{-1}$, which are higher than those found for pillared Chlor−SnP (S_{BET} < 230 $m^2\,g^{-1}$) and fluorinated pillared Al−ZrP solids (S_{BET} < 185 $m^2\,g^{-1}$ and $\sum V_p$ < 0.27 $cm^3\,g^{-1}$). The mesoporous character of the Al−SnP

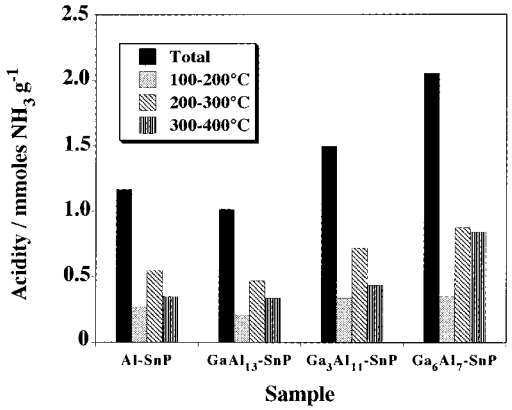

Figure 9. Total acidity of fluorinated calcined solids from NH_3 TPD: (a) Al−SnP, (b) $GaAl_{13}$−SnP, (c) Ga_3Al_{11}−SnP, and (d) Ga_6Al_7−SnP.

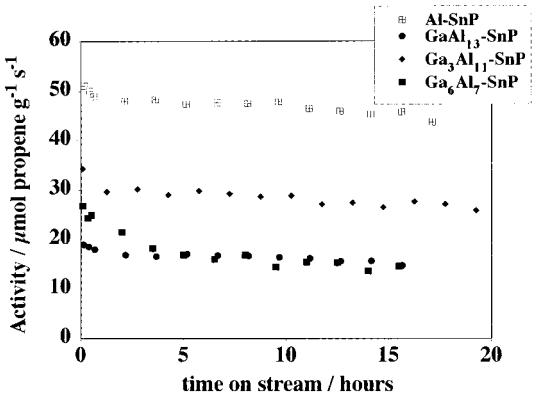

Figure 10. Catalytic activity of fluorinated pillared materials in the decomposition of 2-propanol as a function of time on stream: (a)−(d) as in Figure 9. Experimental conditions: atmospheric pressure; T = 220 °C; feed mixture, isopropyl alcohol/He; alcohol concentration, 11.3 vol %.

solid is attributed to platelet stacking or end−end particle interactions, while the microporosity comes from interlayer cavities induced by pillaring. The increase in specific surface area of fluorinated Al− and Ga/Al−SnP solids in comparison to Chlorhydrol−SnP is related to the presence of oligomeric species with higher nuclearity and stability in the interlayer region, whereas the differences with the fluorinated Al−ZrP materials are rather related to the strength of interaction between the phosphate layer and the intercalated species. The presence of larger species in the interlayer results in a greater microporosity (V_μ = 0.064−0.104 $cm^3\ g^{-1}$) for the pillared materials, reaching a micropore volume of 0.1 $cm^3\ g^{-1}$, close to those reported for pillared clays.[1e] Typical pore size distributions, determined by the Cranston and Inkley method, are also shown in Figure 8. Narrow distributions were found with most of the pores having radii in the range 16−22 Å.

The acidity of the pillared materials has been evaluated by temperature-programmed desorption of ammonia between 100 and 400 °C. Values of total acid sites range between 1, for Al−SnP, and 2 mmol $NH_3\ g^{-1}$, for Ga_6Al_7−SnP; i.e., the acidity increases with Ga content (Figure 9). The substitution of Al by Ga in octahedral sites of the clusters increases, therefore, the acidity of the oxide pillars. Ammonia is mainly desorbed between 200 and 300 °C, which is indicative of the presence of acid sites with medium strength in all materials. In addition, strong acid sites (ammonia desorption between 300 and 400 °C) are also detected for Ga_6Al_7−SnP. The total acidity of these materials is higher than that of pillared clays[24] but lower than that of fluorinated Al−ZrP.[9]

The reaction of decomposition of isopropyl alcohol has been used in order to evaluate the acid properties of the catalytic sites of the fluorinated Al− and Ga/Al oxide pillared tin phosphate solids. Figure 10 shows the catalytic activity of pillared solids as a function of time on stream. In all cases, the catalytic activity was almost stable for at least 20 h of reaction time, and propylene (dehydration reaction) was the only reaction product, demonstrating the exclusive presence of acid sites in these solids. Strikingly, the Al−SnP material exhibits an activity (46 μmol $g^{-1}\ s^{-1}$) much higher than that of its homologue Al−ZrP (23.7 μmol $g^{-1}\ s^{-1}$ as maximum).[9] This enhanced activity may be due to both a higher proportion of Lewis acid sites and higher BET surface area. Among the mixed Ga/Al−SnP solids, the most active was Ga_3Al_{11}−SnP (26 μmol $g^{-1}\ s^{-1}$), which presents the highest basal expansion and BET surface area values. The rest of the materials provide values of catalytic activity close to 15 μmol $g^{-1}\ s^{-1}$. Similarly, Ga-pillared clays appear to be slightly less acidic catalysts than their Al homologues for hydroconversion of *n*-heptane.[24] The activity of the studied catalysts is not only dependent on the chemical nature of the materials but also on the textural characteristics, since a good relationship between catalytic activity and pore volume is found, indicating that the confinement effect in pores influences the catalytic decomposition of isopropyl alcohol molecules.

Conclusions

Fluorinated aluminum and mixed gallium/aluminum oligomers of higher nuclearity than the species Al_{13}^{7+} have been intercalated into colloidal α-tin phosphate. These intercalated materials are thermally more stable and lead to fluorinated aluminum and mixed gallium/aluminum oxide pillared materials with higher free heights, and hence higher interlayer porosity, than those prepared from solutions of Al_{13}^{7+}. ^{31}P and ^{27}Al MAS NMR studies have revealed that strong interactions between the phosphate layer and the intercalated species are established upon calcination. The appearance of low coordination sites of aluminum in calcined materials points to aluminum and mixed gallium/aluminum oxide nanoparticles that are cross-linked to the phosphate layer, through Al−O−P bonds. These sites may act as Lewis acid centers and could be mainly responsible for the high acidity displayed by the oxide pillared materials, which behave exclusively as dehydrating catalysts for the decomposition of isopropyl alcohol.

Acknowledgment. This research was supported by the CICYT (Spain) Project MAT 97-906. P.B.-G. thanks the Junta de Andalucía for a fellowship. The authors thank Dr. M. D. Alba-Carranza for recording MAS NMR spectra.

References and Notes

(1) (a) Brindley, G. W.; Sempels, R. E. *Clay Miner.* **1977**, *12*, 229. (b) Vaughan, D. E. W.; Lussier, R. J. *Proceedings of the 5th International Conference on Zeolites*, Naples, Italy; Ress, L. V. C., Ed.; Heyden Press: Chichester, 1980. (c) Lahav, N.; Shani, V.; Shabtai, J. *Clays Clay Miner.* **1978**, *26*, 107. (d) Pinnavaia, T. J.; Tzou, M. S.; Landau, S. D.; Raythatha, R. H. *J. Mol. Catal.* **1984**, *27*, 195. (e) Tichit, D. Ph.D. Thesis, Université de Montpellier, 1986. (f) Hardin, S.; Hay, D.; Millikan, M.; Sanders, J. V.; Turney, T. W. *Chem. Mater.* **1991**, *3*, 977. (g) Lambert, J. F.; Chevalier, S.; Franck, R.; Suquet, H.; Barthomeuf, D. *J. Chem. Soc., Faraday Trans.* **1994**, *90*, 667. (h) Vaughan, D. E. W. In Burch, R., Ed. *Catalysis Today, Pillared Clays;* Elsevier: Amsterdam, 1988; p 187.

(2) (a) Clearfield, A.; Roberts, B. D. *Inorg. Chem.* **1988**, *27*, 3237. (b) Olivera-Pastor, P.; Jiménez-López, A.; Maireles-Torres, P.; Rodríguez-Castellón, E.; Tomlinson, A. A. G.; Alagna, L. *J. Chem. Soc., Chem. Commun.* **1989**, 751.

(3) (a) Wong, S.-T.; Cheng, S. *Inorg. Chem.* **1992**, *31*, 1165. (b) Mohan Ram, R. A.; Clearfield, A. *J. Solid State Chem.* **1994**, *112*, 288. (c) Nazar, L. F.; Jacobson, A. J. *J. Mater. Chem.* **1994**, *4*, 1419.

(4) Johansson, G. *Acta Chem. Scand.* **1960**, *14*, 769.

(5) (a) Bradley, S. M.; Kydd, R. A.; Yamdagni, R. *J. Chem. Soc., Dalton Trans.* **1990**, 2653. (b) Bradley, S. M.; Kydd, R. A.; Yamdagni, R. *Magn. Reson. Chem.* **1990**, *28*, 746. (c) Bradley, S. M.; Kydd, R. A.; Fyfe, C. A. *Inorg. Chem.* **1992**, *31*, 1181.

(6) (a) Bradley, S. M.; Kydd, R. A. *Catal. Lett.* **1991**, *8*, 185. (b) González, F.; Pesquera, C.; Blanco, C.; Benito, I.; Mendioroz, S. *Inorg. Chem.* **1992**, *31*, 727. (c) Kloprogge, J. T.; Booy, E.; Jansen, J. B. H.; Geus, J. W. *Clay Miner.* **1994**, *29*, 153. (d) Tang, X.; Xu, W.-Q.; Shen, Y.-F.; Suib, S. L. *Chem. Mater.* **1995**, *7*, 102. (e) Bagshaw, S. A.; Cooney, R. P. *Chem. Mater.* **1995**, *7*, 1384. (f) Hernando, M. J.; Pesquera, C.; Blanco, C.; Benito, I.; González, F. *Chem. Mater.* **1996**, *8*, 76.

(7) (a) Alberti, G.; Costantino, U. In *Intercalation Chemistry*; Whittingham, M. S., Jacobson, A. J., Eds.; Academic Press: New York, 1982; pp 147−180. (b) Clearfield, A. *Comments Inorg. Chem.* **1990**, *10*, 89.

(8) Olivera-Pastor, P.; Maireles-Torres, P.; Rodríguez-Castellón, E.; Jiménez-López, A.; Cassagneau, T.; Jones, D. J.; Rozière, J. *Chem. Mater.* **1996**, *8*, 1758.

(9) Mérida-Robles, J. M.; Olivera-Pastor, P.; Jiménez-López, A.; Rodríguez-Castellón, E. *J. Phys. Chem.* **1996**, *100*, 14726.

(10) Costantino, U.; Gasperoni, A. *J. Chromatogr.* **1970**, *51*, 289.

(11) Fu, G.; Nazar, L. F.; Bain, A. D. *Chem. Mater.* **1991**, *3*, 602.

(12) Cranston, R. W.; Inkley, F. A. *Adv. Catal.* **1957**, *9*, 143.

(13) (a) Maireles-Torres, P.; Olivera-Pastor, P.; Rodríguez-Castellón, E.; Jiménez-López, A.; Alagna, L.; Tomlinson, A. A. G. *J. Mater. Chem.* **1991**, *1*, 319. (b) Maireles-Torres, P.; Olivera-Pastor, P.; Rodríguez-Castellón, E.; Jiménez-López, A.; Tomlinson, A. A. G. *J. Solid State Chem.* **1991**, *94*, 368.

(14) Alberti, G.; Marmottini, F. *J. Colloid Interface Sci.* **1993**, *157*, 513.

(15) Parker, W. O., Jr.; Millini, R.; Kiricsi, I. *Inorg. Chem.* **1997**, *36*, 571.

(16) Hudson, M. J.; Workman, A. D. *J. Mater. Chem.* **1991**, *1*, 375.

(17) Rodríguez-Castellón, E.; Olivera-Pastor, P.; Maireles-Torres, P.; Jiménez-López, A.; Sanz, J.; Fierro, J. L. G. *J. Phys. Chem.* **1995**, *99*, 1491.

(18) MacLachlan, D. J.; Morgan, K. R. *J. Phys. Chem.* **1990**, *94*, 7656.

(19) Paparazzo, E.; Severini, E.; Jiménez-López, A.; Maireles-Torres, P.; Olivera-Pastor, P.; Rodríguez-Castellón, E.; Tomlinson, A. A. G. *J. Mater. Chem.* **1992**, *2*, 1175.

(20) Moulder, J. F.; Stickle, W. F.; Sobol, P. E.; Bomben, K. D. *Handbook of X-ray Photoelectron Spectroscopy*; Chastain, J., Ed.; Perkin-Elmer Corp.: Minnesota, WI, 1992.

(21) Nazar, L. F.; Fu, G.; Bain, A. D. *J. Chem. Soc., Chem. Commun.* **1992**, 251.

(22) Coster, D.; Fripiat, J. J. *Chem. Mater.* **1993**, *5*, 1204.

(23) Mortlock, R. F.; Bell, A. T.; Radke, C. J. *J. Phys. Chem.* **1993**, *97*, 775.

(24) Zubkov, S. A.; Kustov, L. M.; Kazansky, V. B.; Fetter, G.; Tichit, D.; Figueras, F. *Clays Clay Miner.* **1994**, *42*, 421.